

Computational Simulations of the King's Plain Wind Farm

Christopher M Cicalla Jr¹, Bryan Mendoza², Ali M Alabadi,³
Brandon Burnett⁴, and Natania Middleton⁵

Department of Mechanical Engineering, University of Memphis, Memphis, Tennessee, 38152,

United States of America

The American Wake Experiment or AWAKEN is an ongoing, landmark international wind turbine and farm wake validation campaign. We plan to show that the King's Plain wind farm can help be at the forefront of renewable energy. There are unanswered questions about the wake dynamics that hinder our ability to optimize wind energy production that can be addressed through targeted experimental and computational analysis. We plan to model the 88-turbine King's Plain wind farm and analyze the wake and its turbulence. We use large-eddy simulation, a high-fidelity computational model, and an actuator disk model to parameterize the wind turbines. The actuator disk model simplifies the representation of a wind turbine in simulations. The ADM represents the turbine as a porous disk that exerts a force on the flow. The simulation is performed on a high-performance computer using distributed memory processing and approximately 30 Sapphire Rapids compute nodes costing over 190,000 CPU hours. The simulation captures the large-scale atmospheric, wind farm, and wind turbine wake features, which are crucial for understanding how power is produced in the wind farm. This force mimics the effect of the turbine extracting energy from the wind. We will investigate wake formation and interaction dynamics of different interaction scenarios that occur in the irregular wind farm layout.

I. Introduction

The global demand for clean and sustainable energy sources is more critical than ever. Wind energy has emerged as a leading renewable energy source, playing a critical role in reducing reliance on fossil fuels. To advance wind energy and decrease its levelized cost of electricity, optimizing the performance and efficiency of wind farms is crucial. However, a significant challenge in wind farm design and operation lies in understanding and predicting wind turbine wake dynamics. These wakes, which are characterized by reduced wind speed and increased downstream of turbines, can significantly impact the power production of further turbines downstream and the overall efficiency of the wind farm.

Wind turbine-to-turbine wake interactions are a major cause of energy production loss, which can account for a 20% to 50% loss on downwind turbines. For example, row-averaged power measurements at the Horns Rev wind farm show a 40% loss in production from the first row to the second row [1]. This is mainly due to the strong velocity deficit created by the upwind turbines, which substantially decreases the average velocity experienced by the

Undergraduate, Department of Mechanical Engineering, Student Member Christopher Cicalla (1603493)

Undergraduate, Department of Mechanical Engineering, Student Member Bryan Mendoza (1400317)

Undergraduate, Department of Mechanical Engineering, Student Member Natania Middleton (1810643)

Undergraduate, Department of Mechanical Engineering, Student Member Brandon N. Burnett (1823363)

Faculty, Department of Mechanical Engineering, Member, Daniel Foti (450024)

downwind turbines. However, there are additional dynamics of turbine-to-turbine wake interactions that influence the energy production uncertainty [2] that can increase the turbulence intensity in the wakes. In order to address the reduction of the levelized cost of electricity from wind power, the effects of turbine-to-turbine interactions must be better understood.

The American Wake Experiment (AWAKEN) is an international, multi-institutional wind field energy campaign designed to help answer the most pressing question on turbine interactions between other turbines and the atmosphere inside the wind farm. The measurement campaigns have included a vast array of sensors and wind turbine monitors covering three different wind farms in north-central Oklahoma. The site is co-located near the US Department of Energy Atmospheric Radiation Measurement Southern Great Plains (SPG) user facility site, which provides continuous monitoring of atmospheric dynamics in the facility. Data from the Kings Plain Site, 88-turbine wind farm, is part of an ongoing modeling validation effort to provide valuable benchmarking data and contribute to a fuller understanding of wake dynamics.

Efforts to study turbine arrays through modeling and simulation are quite extensive. Many focus on the mean velocity and flow structure to investigate the average power production of an array or site. More recently, the dynamics of the turbine wakes and the wind farm-induced structures as well as optimization of turbine array layouts, have been conducted. Site-specific validation of modeling is often difficult due to the proprietary nature of the commercialization of wind energy. However, measurements from the AWAKEN project enable validation and benchmarking effects of different modeling approaches to be assessed.

In this work, we employ a high-fidelity, large-eddy simulation (LES) approach to the full King's Plain wind farm. The primary objective of this project is to model the spatio-temporal wake and farm dynamics of the 88 turbines and analyze the resulting wake formations and interaction dynamics. By employing LES, a technique capable of capturing large-scale turbulent features, this study aims to provide detailed insights into the complex wake behavior within a large-scale wind farm. Simulations are run on HPCs (high-performance computing) resources, using distributed memory processing to handle the computational demands of this large-scale problem. We describe the large-eddy simulations and turbine parameterization in section II and the simulation setup in section III. The results in section IV will present the analysis of the wind farm and select turbines. Finally, we summarize the work in section V.

II. Numerical Methods

The computational investigation employs the Virtual Wind Simulator (VWiS) with the curvilinear immersed boundary method (CURVIB), which has been used successfully in a wide range of airfoil and moving blade analyses [2-5]. The solver is based on incompressible Navier-Stokes equations in generalized curvilinear coordinates. The governing equations are discretized on a hybrid staggered/non-staggered grid using three-point central finite differencing and integrated in time via a second-order accurate fractional step method. The continuity and momentum equations are as follows:

$$\frac{\partial U_i}{\partial \xi_i} = 0$$

$$\frac{1}{J} \frac{\partial U_i}{\partial t} = \frac{\partial}{\partial \xi_j} \left(-\frac{1}{\rho} \xi_i^l \frac{\partial p}{\partial \xi_l} + \frac{1}{J} \tau_{ij}' - U_j u_i' \right) + \frac{\mu}{\rho} \frac{\partial}{\partial \xi_j} \left(\frac{1}{J} g^{jk} \frac{\partial u_l}{\partial \xi_k} \right),$$

where $\xi_i^l = \partial \xi_i / \partial x_l$ are the transformation metrics, J is the Jacobian of the geometric transformation, u_i is the i th component of the velocity vector in Cartesian coordinates, $U_i = (\xi_i / J)$ is the contravariant volume flux, $g_{jk} = \xi_j \cdot \xi_k$ are the components of the contravariant metric tensor, ρ is the density, μ is the dynamic viscosity, p is the pressure, τ_{ij} represents the anisotropic part of the sub grid-scale stress tensor. A dynamic subgrid-scale model is employed using the dynamic Smagorinsky model [6,7].

The actuator disk model offers a computationally efficient approach to represent wind turbines in simulations, making it particularly useful for large-scale wind plant computations. However, its simplicity comes at the cost of reduced physical accuracy, as it does not capture the detailed flow phenomena around the blades and near the rotor. Despite these limitations, the actuator disk model has played a crucial role in advancing the understanding of wind

turbine wakes and the optimization of wind plant layouts. Following one-dimensional blade element momentum theory, the thrust force F_T exerted by wind on the disk is given by

$$F_T = \frac{1}{2} \rho C_T U_\infty^2 \frac{\pi}{4} D^2$$

where C_T is the imposed wind turbine thrust coefficient and U_∞ is the incoming velocity.

III. Case Setup

The AWAKEN campaign takes place in Northern Oklahoma near the DOE Atmospheric Radiation Measurement (ARM) Program's Southern Great Plains (SGP) user facility site. The King's Plain wind farm has 88 GE 2.82 MW turbines operating over an approximately 15 km x 15 km region. The turbines have a height $H=88$ m and diameter $D=127$ m. At the optimal operating conditions at a tip-speed ratio of 10, the $C_T=0.7479$. We based our simulations on conditions on 24 Aug 2023 between 05:00 and 07:00 UTC.

The average wind direction at this time comes from the southeast. In order to include all 88 wind turbines in their irregular layout, the computational domain is set to be $L_x \times L_y \times L_z = 15 \text{ km} \times 1 \text{ km} \times 15 \text{ km}$. The computational domain is discretized with uniform spacing in the streamwise and spanwise directions of $N_x \times N_y \times N_z = 1850 \times 50 \times 1850$. The vertical velocity is stretched such that around the turbine $\Delta y/D = 20$. The average bulk streamwise velocity is set to be $U_b = 10$ m/s and boundary layer height $\delta = 1.5D$, which sets the bulk Reynolds number $Re = U_b \delta/\nu = 1.2 \times 10^8$. The friction velocity is approximately $u^*/U_b = 0.47$ with roughness height $z_i = 0.05$ m on the wall.

A precursor simulation is run to create turbulent inflow conditions based on measurements on 24 Aug 2023 between 05:00 and 07:00 UTC. The 5 km x 1 km x 15 km domain is used to impose create an unsteady turbulent inflow to the wind farm domain. Figure 1(a) shows the streamwise velocity averaged in time and across the spanwise inflow plane. The boundary layer height is around 1.5 diameters above the ground. The wind speed above the turbine decreases to a contain velocity around 60% of the maximum velocity. The turbulence levels in the inflow are shown through the streamwise-vertical Reynolds stresses in Fig. 1(b). The wall shear layer and the top shear layer formed about the surface layer that forms.

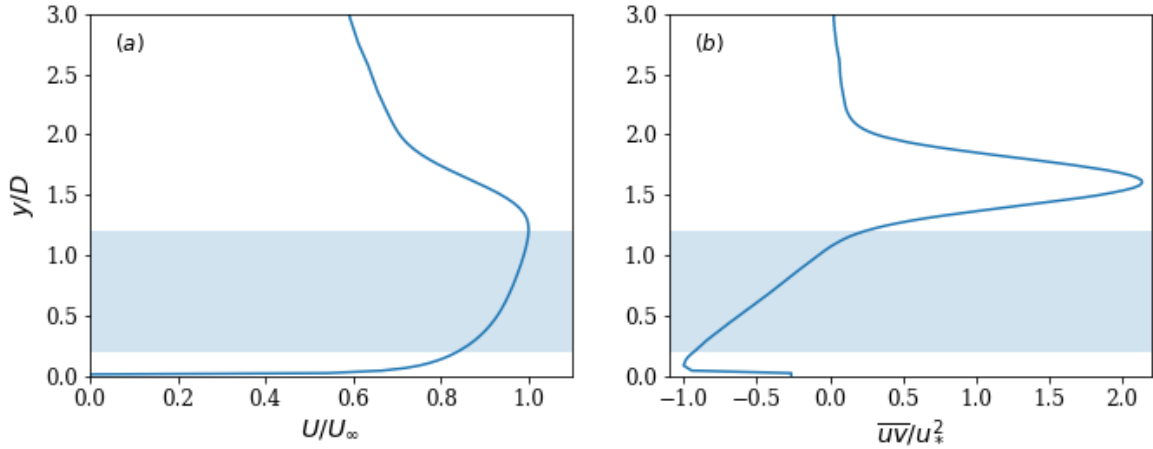


Figure 1: (a) Average inflow streamwise velocity U normalized by maximum velocity and (b) streamwise-vertical Reynolds stress normalized by friction velocity.

IV. Results

Figure 2 shows the layout of the 88 wind turbines at the King's Plain wind farm with the wind coming from the southeast. In Fig. 2(a) and (b), we are overhead looking at both the average streamwise velocity and the velocity variance at hub height, respectively. Here, we can see the wake average behind the turbines. As we go further downstream, we can see a decrease in velocity. The front row of turbines takes, depending on conditions and assuming the most efficient, up to 50% of the energy out of the incoming flow and leaves little for the downstream turbines.

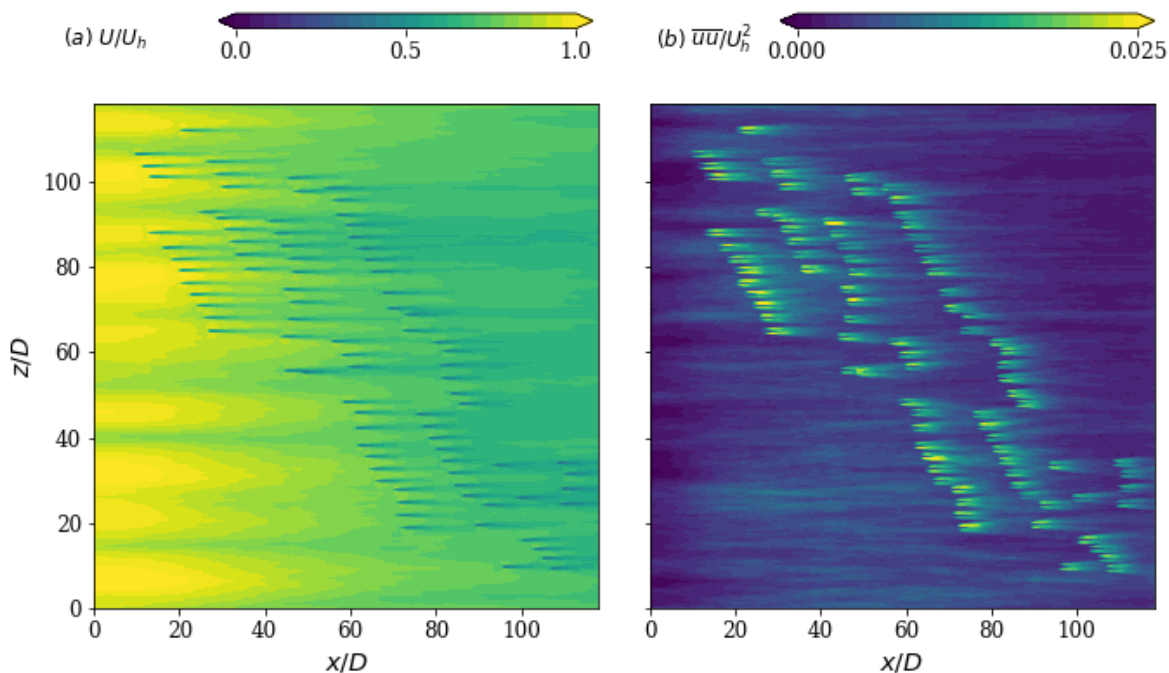


Figure 2: (a) Average streamwise velocity and (b) streamwise velocity variance at hub height for the King's Plain wind farm.

Average streamwise velocity is the mean velocity of parallel flow to the main flow. It is a crucial parameter in fluid dynamics as it influences flow downstream. Understanding how it affects the downstream flow is crucial in predicting the efficiency and performance of wind turbines. As we see, the incoming flow is nice and strong, but once it gets to the turbines, the velocity drops considerably. There are many varied factors to look at i.e., wake effect, wake meandering, and tip vortices. These lead to power fluctuations, and the higher the variance, the greater the power fluctuation. This also shifts the power load intermittently throughout the downstream turbines.

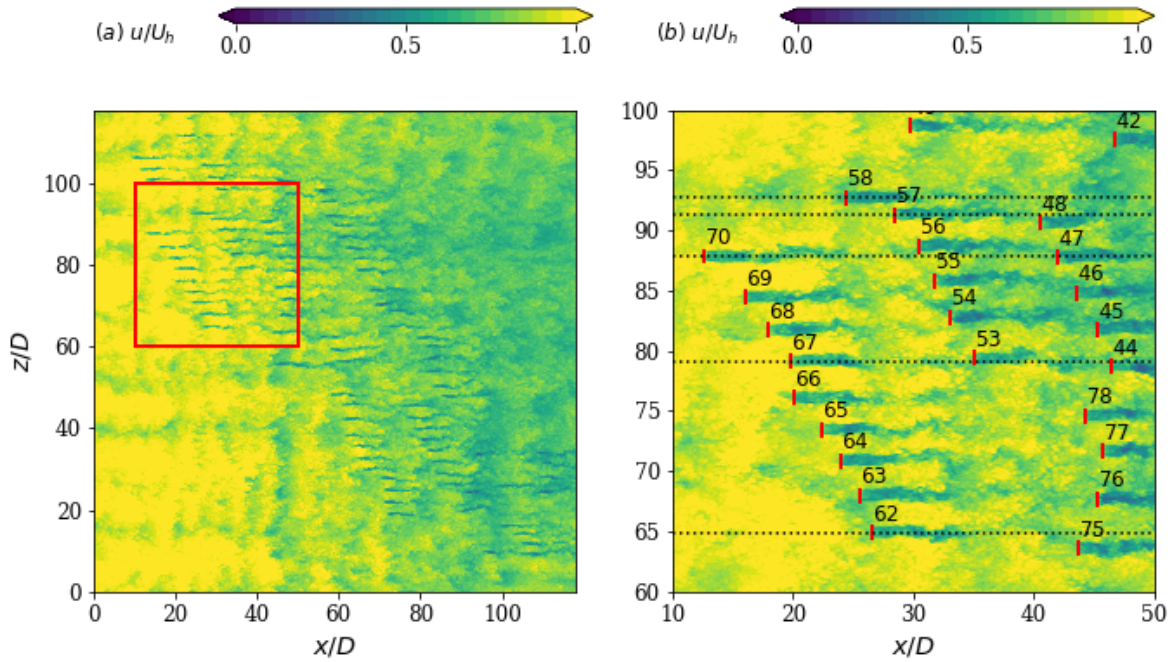


Figure 3: (a) Instantaneous streamwise velocity at hub height. (b) Zoom-in view of the red region. Horizontal lines correspond to slices through turbines for analysis below.

Figure 3 shows the instantaneous velocity, which shows the wake dynamics of the unsteadiness of the incoming flow, turbine wakes, and wake meandering. Wake meandering is a far wake phenomenon where the wake undergoes periodic spanwise oscillations. Figure 3(b) is zoomed into an upwind region for further analysis. Five vertical slices of the wind farm are selected for further analysis. Row start with turbine 62 is chosen on the end and doesn't have turbine downwind. Turbine 67 is chosen because it's confined between turbines 66 and 68 and there are turbines downwind. Turbine 70 is the most upwind turbine and unaffected by other turbines. Turbines 57 and 58 are chosen close together.

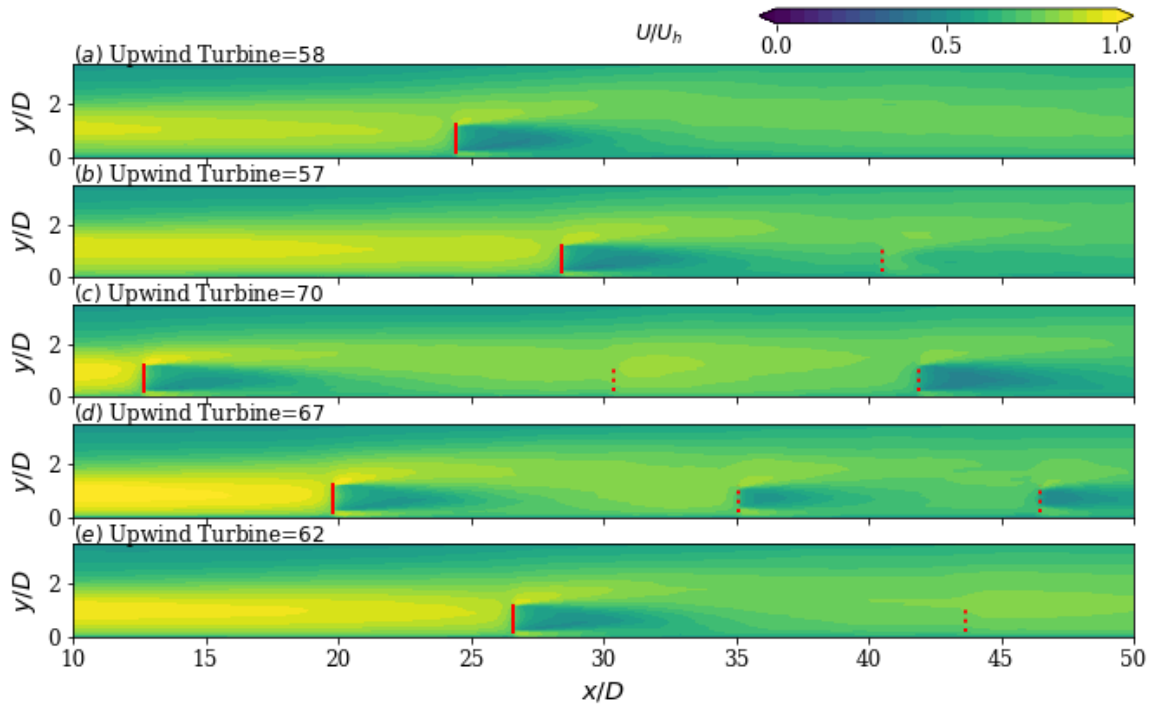


Figure 4: Instantaneous streamwise velocity on planes centered on upwind turbines 58, 57, 70, 67, and 62. The red lines represent the upwind turbine rotor. Red dashed lines are downwind turbines.

Now we look at the five different turbines that were selected based on Fig. 3. Each one of these turbines offers a new scenario to assess turbine-to-turbine interactions. Figure 4(a) shows the average velocity of the upwind turbine 58. This turbine experiences the inflow velocity from the atmospheric boundary layer and very little interaction with other turbines except for turbine 57, which is slightly downstream. The wake formed by turbine 58 is relatively strong and unaffected by other turbines. In Fig. 4(b), the average velocity in the wake upwind turbine 57 is similar. From the average velocity, it is difficult to see any dynamics of the effects between turbines 57 and 58. In Fig. 4(c), upwind turbine 70 has several turbines downwind. It can be seen that the downwind turbine directly in its path has a weaker velocity deficit, which indicates a lower power production. In a similar scenario, upwind turbine 67 has a large effect on two downwind turbines where the velocity progressively becomes weaker due to the power extraction from the upwind turbines. Similar to upwind turbine 58, the mean velocity deficit in upwind turbine 62 in Fig. 4(e) is not greatly affected by neighboring wind turbines. In both Fig. 4(c) and (e) there is an acceleration of the wake due to offset turbines, which direct more mass flow between neighboring turbines.

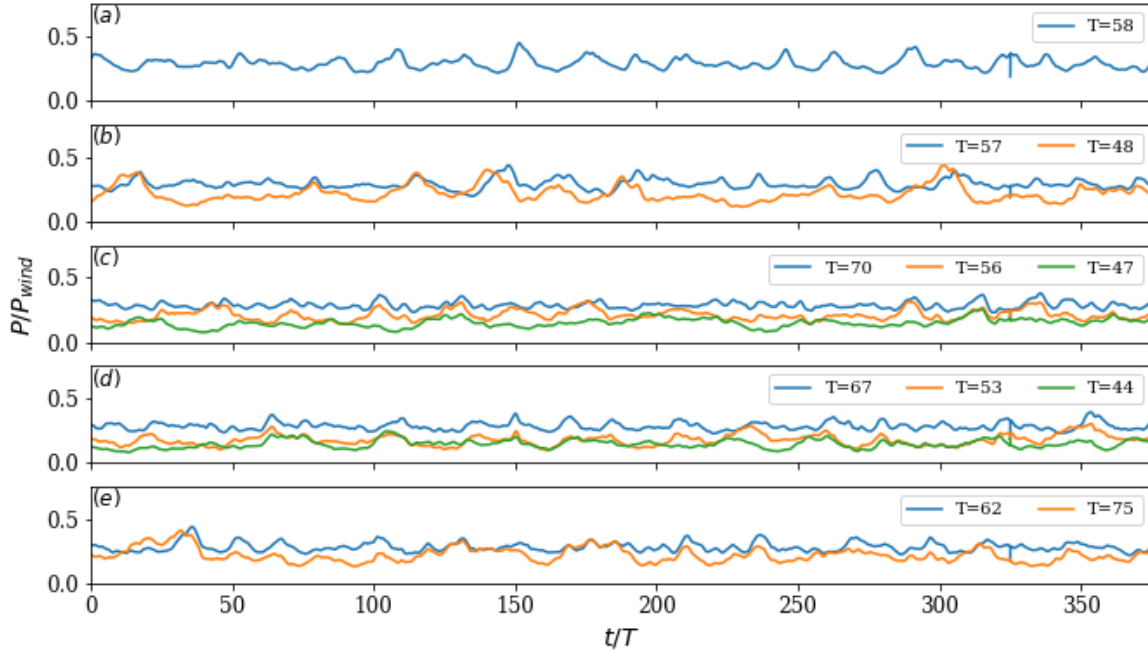


Figure 5: Instantaneous power coefficient for upwind turbines 58, 57, 70, 67, 62.

Figure 5 shows the instantaneous power coefficient of select wind turbines. The power coefficient changes over time, where a more fluctuating line represents an uneven performance of the turbine due to variations in the incoming velocity, and a steadier line represents a more consistent power output. Turbines like 70 and 57 have higher and more steady power outputs, suggesting that their positions are more upstream, leading to lower wake interference. Turbines like 48 and 75 have more fluctuating power outputs due to wake turbulence from their location, suggesting that they are more downstream than the previous turbines.

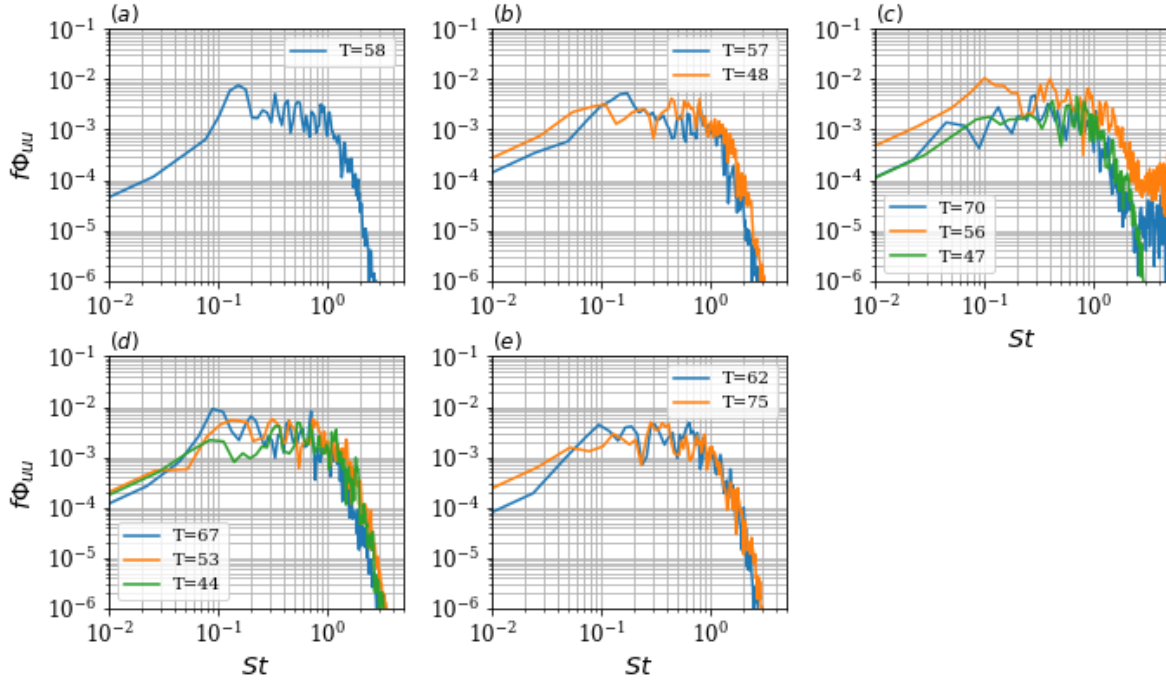


Figure 6: Premultiplied power spectral density at $x/D = 4$ downwind of each turbine. for upwind turbines 58, 57, 70, 67, 62.

The spectral signature of the wakes of the turbines can be examined through the power spectral density (PSD), as shown in Fig. 6. The pre-multiplied PSD allows us to examine common Strouhal numbers and frequency modes across different turbines operating in different conditions based on their location in the wind farm. Fig. 6(a) shows the pre-multiplied PSD for turbine 58. There are several low-frequency peaks present in the spectrum. A major mode occurs around a Strouhal number between 0.15. This Strouhal number is a signature of wake meandering, a large spanwise oscillation of the wake. Wake meandering has a strong effect on the power uncertainty and the turbulence levels experienced by downwind turbines. In Fig. 6(b), the two turbines are shown an upwind turbine 57 and a downwind, but offset, turbine 48. They have a similar spectrum because downwind turbine 48 is offset and experiences a relatively unimpacted incoming velocity from the inflow. On the other hand, in Fig. 6(c), the upwind turbine 70 has a large impact on the downwind turbines 56 and 47. Both downwind turbines are directly behind turbine 70, and a large velocity deficit impacts the turbulence levels. The dynamics of wake meandering generate additional frequency modes in the downwind turbines. A combination of effects observed in Fig. 6(b) and (c) are present in Figure 6(d) where the upwind turbine 67 has an impact on the downwind turbines where one is offset and the other is directly behind the energy levels are similar for the offset turbine while there is a decrease in the turbulence density for the turbine 44. Wake meandering is present in all cases, as evident through Fig. 3 as well as where strong intensity spanwise dynamics are shown in the instantaneous velocity. However, due to the location of the spectra and the actuator disk model, there are no upwind vortical features, such as tip vortices or the hub vortex, present in the energy signature. At this location in the wake, these near-field features will have broken down and dissipated. Overall, the differences between upwind turbines are mostly minimal regardless of potential spanwise interactions. Downwind turbines vary based on their location behind the turbine. The offset turbines experience velocity unimpeded or accelerated through upwind turbines.

V. Conclusion

We employed LES to investigate the King’s Plain wind farm, which consists of 88 turbines. The simulation is performed on a high-performance computer using distributed memory processing and approximately 30 Sapphire Rapids compute nodes costing over 190,000 CPU hours. Due to the size of the domain, this cost is significant to capture the unsteady wind dynamics. We looked at five different turbine conditions based on layout. The upwind turbines behaved mostly similarly, while downwind turbines operated differently based on incoming conditions. In the future, results will be directly compared to the benchmarks established by the AWAKEN project, contributing to the validation of computational models for wind farm wake predictions and furthering thunderation of wake physics in complex wind farm environments.

Acknowledgments

This work is supported by the National Science Foundation under Grant No. 21-36371. This work used Texas Advanced Computing Center (TACC) The University of Texas at Austin and Anvil at Purdue University through allocation PHY220038 from the Advanced Cyberinfrastructure Coordination Ecosystem: Services & Support (ACCESS) program, which is supported by National Science Foundation Grants No. 21-38259, No. 21-38286, No. 21-38307, No. 21-37603, and No. 21-38296.

References

- [1] Barthelmie, R. L, et al, Modelling and measurements of wakes in large wind farms. *J. Phys. Conf. Ser.* 75 (1) 2007, ,012049.
- [2] Foti, D., Yang, X., Guala, M., and Sotiropoulos, F., “Wake meandering statistics of a model wind turbine: Insights gained by large eddy simulations,” *Physical Review Fluids*, Vol. 1, No. 4, 2016, p. 044407.
- [2] Foti, D., Yang, X., and Sotiropoulos, F., “Similarity of wake meandering for different wind turbine designs for different scales,” *Journal of Fluid Mechanics*, Vol. 842, 2018, pp. 5–25.
- [3] Foti, D., Yang, X., Campagnolo, F., Maniaci, D., and Sotiropoulos, F., “Wake meandering of a model wind turbine operating in two different regimes,” *Phys. Rev. Fluids*, Vol. 3, No. 5, 2018, p. 054607.
- [4] Foti, D., Yang, X., Shen, L., and Sotiropoulos, F., “Effect of wind turbine nacelle on turbine wake dynamics in large wind farms,” *Journal of Fluid Mechanics*, Vol. 869, 2019, pp. 1–26.
- [5] Smagorinsky, J., “General circulation experiments with the primitive equations: I. The basic experiment,” *Monthly Weather Review*, Vol. 91, No. 3, 1963, pp. 99–164.
- [6] Germano, M., Piomelli, U., Moin, P., and Cabot, W. H., “A dynamic sub grid-scale eddy viscosity model,” *Physics of Fluids A: Fluid Dynamics*, Vol. 3, No. 7, 1991, pp. 1760–1765.